Journal of the Taiwan Institute of Chemical Engineers 117 (2020) 182–189

Contents lists available at ScienceDirect

Journal of the Taiwan Institute of Chemical Engineers

journal homepage: www.elsevier.com/locate/jtice

Struvite production from dairy processing wastewater: Optimizing reaction conditions and effects of foreign ions through multi-response experimental models

Claver Numviyimana*, Jolanta Warchoł, Grzegorz Izydorczyk, Sylwia Baśladyńska, Katarzyna Chojnacka

Department of Advanced Material Technology, Faculty of Chemistry, Wrocław University of Science and Technology, ul. M. Smoluchowskiego 25, Wrocław 50-372, Poland

ARTICLE INFO

Article History:
Received 31 August 2020
Revised 9 November 2020
Accepted 28 November 2020
Available online 3 December 2020

Keywords:
Phosphorus recovery
Struvite precipitation
Multi-response
Desirability
Counterions effect
Nutrients release kinetics

ABSTRACT

Struvite is the preferred form of phosphorus recovery for fertilizer by chemical precipitation. The concentration of phosphorus in raw wastewater from dairy processing is higher than acceptable values for prevention of water pollution. Along with phosphorus, potassium and calcium are its main counterions with high concentration. Thus, calcium phosphate salts are prompt to precipitate and decrease struvite production. The effect of such phosphate counter-ions were optimized using design of experiments and desirability function to maximize both phosphorus recovery and struvite production. Under optimum conditions, the yields were 98.6 ± 1.1 and 85.7 ± 2.5 percent for phosphorus recovery and struvite precipitation, respectively. Factors optimization was achieved with desirability D = 0.995. By in-vitro assay of nutrients release, the product demonstrated better phosphorus availability than the one obtained with high calcium dose in reactor. The obtained molar ratios of dose can serve in wastewater treatment coupled to phosphorus precipitation with a fertilizer value product.

1. Introduction

Phosphorus (P) fate has been a claim in environmental, economic and agriculture domains [1]. The latter is reported among soil nutrient depletion, a root cause of the decrease in crop production [2]. Water bodies and biota are facing eutrophication caused by excess of phosphates from industrial effluents [3–6]. As mitigation measures, the P recovery from wastewater is interesting thematic research in agricultural, environmental and chemical engineering. The usual process of P removal in waste water treatment plants (WWTP) involves biological processes and chemical precipitation of inorganic P. The latter is done by additional dosing of either iron or calcium salts which precipitate P to iron and calcium phosphates [7,8]. In this chemical process, the inorganic P is efficiently removed. Nevertheless, the salts thereby precipitated are of lower quality for use as P fertilizer due to their lower P availability to plant [9]. Struvite is the preferred form of P recovery for use as inorganic fertilizer considering its provision of P and nitrogen in efficiently available form for plant nutrition [10]. Struvite chemically named as magnesium ammonium phosphate hexahydrate (MAP) is formed in a supersaturated aqueous solution with Mg^{2+}, NH_4^+, and PO_4^{3-} according to the reaction described by Eq. (1).

$$Mg^{2+}_{(aq)} + NH_4{}^+_{(aq)} + H_nPO_4{}^{(3-n)-}_{(aq)} + 6H_2O_{(l)} \rightleftharpoons MgNH_4PO_4 \cdot 6H_2O_{(s)} + nH^+_{(aq)} \quad (1)$$

Besides magnesium, multi-components aqueous matrices contain more phosphate counterions able to pair with phosphate and form less soluble salts [11]. This makes a counter competition with magnesium and ammonium during struvite precipitation with possibility of its full inhibition [12]. Calcium effect was pointed out in several researches where its high level favors precipitation of its salts including calcium phosphate ($Ca_3(PO_4)_2$, $K_{sp} = 2.07 \cdot 10^{-33}$), hydroxyapatite ($Ca_5(PO_4)_3OH$, $K_{sp} = 2.1 \cdot 10^{-58}$), octacalcium phosphate ($Ca_8H_2(PO_4)_6 \cdot 5H_2O$, $K_{sp} = 1.12 \cdot 10^{-48}$), and dicalcium phosphate [13,14]. Though there are other phosphate counterions including aluminum, copper, cadmium, iron and other multivalent metals, they are in trace levels in milk processing effluents [15]. Thus, calcium at higher molal concentration than magnesium remains the main phosphate counter ion with high precipitation potential to inhibit struvite ($K_{sp} = 10^{-13.6}$) in non-optimized conditions [16]. Shalaby et al. carried out Ca^{2+} removal prior to struvite precipitation for P recovery as struvite [17]. Moreover, Wang et al. studied the effect of ion molar ratios in P removal where calcium increased the P recovery with adverse effect

* Corresponding author.
E-mail address: claver.numviyimana@pwr.edu.pl (C. Numviyimana).

https://doi.org/10.1016/j.jtice.2020.11.031

on fertilizer quality [18]. In non-optimized conditions, struvite may be formed at an extent depending on its supersaturation level. However, the content in product is decreased by various multivalent metals. Marti et al. assessed struvite precipitation during anaerobic digestion process where only 58% of struvite content was found in product, the remaining being mainly amorphous calcium phosphate salts [19]. Furthermore, struvite forms were alternatively discussed for co-precipitation with K-struvite (K_{sp} = $2.4{\cdot}10^{-11}$) depending on super-saturation of either ammonium or potassium with the possibility of formation of both compounds in solid phase [20]. On the other hand, a number of researches was previously done on P recovery by struvite precipitation from various wastes [21] including urine [22], cow manure [23], and industrial waste water [17,24,25]. However, researches on P recovery in form of struvite from dairy processing wastes are limited. Moreover, dairy products are a major source of calcium, thus the wastewater from milk processing has high level of calcium and its removal for struvite production is an excessive work and additional cost [26]. In this work, cheese production wastewater (whey) was used to study the optimum pH and salts dosage for P recovery as fertilizer with high struvite content. Several approaches have been previously used including computation methods, as well as experimental methods by factors optimization with one focus of P removal [27]. This work aimed the use of multi-response optimization of reaction conditions and the effects of foreign ions to recover P with high struvite content from liquid whey. The resulting products were evaluated for fertilizer quality using kinetic models based on *in-vitro* nutrients release.

2. Material and methods

2.1. Chemicals and reagents

Magnesium sulfate, di-potassium phosphate, anhydrous calcium chloride, sodium hydroxide, and ammonium chloride were used as magnesium, P, calcium and alkali source, respectively. All reagents with a purity 99.5% were obtained from Avantor Performance Materials Poland S.A. Deionized water was produced in laboratory demineralization system Millipore Simplicity UV (Merck, Germany). Nitric acid (65%), hydrogen peroxide (30%), and sulphuric acid (>95%) (Avantor Performance Materials Poland S.A., Poland) were used in sample mineralization and cleaning materials. Multi-element standard (ULTRA Scientific, USA) was used for standard calibration in ICP-OES analysis. Boric acid, mixed indicator of green bromocresol and methyl red; mixt catalyst (K_2SO_4, $CuSO_4$, Se, $FeSO_4$), and hydrochloric acid analytical weight for 1 L 0.1 N were used in total nitrogen digestion, ammonium collection and titration, respectively.

2.2. Sample collection and analysis

Waste water from cheese production was collected from local factory of cheese production — The District Dairy Cooperative in Krzepice, Poland. Sampling materials were 5 L high density polyethylene bottles cleaned with sulphuric acid and rinsed with de-ionized water.

2.3. Instrumentation

Sample mineralization was done by microwave digestion system (Start D, Milestone) followed by multi-elemental analysis with inductively coupled plasma optical emission spectrometer (ICP- OES Vista MPX, Varian). The concentration of anions was determined by ion chromatography (ICS-1100 Dionex Corporation). Kjeldhal digestion and distillation units together with digital burette served for total nitrogen sample digestion, ammonium distillation, and titration, respectively. Total and organic carbon were analysed using macro combustion analyser (Vario Macro Cube elementary analyser GmbH, made in Germany). Precipitation experiments were conducted in batch reactors equipped with 1 L beaker, water bath with temperature regulation (Type: PLWC 35S made in Poland), and up stirrer (CAT-100, made in Germany) with time and stirring rate control settings. Multifunction meter CX-705 Elemtron was used in pH measurement. The X-ray refractometer (Empyrean, PANanalytical) and scanning electron microscopy (SEM/Xe-PFIB Microscope FEI Helios PFIB) were utilized for product X-ray diffraction (XRD) analysis and imaging, respectively.

2.4. Procedure

The composite sample was characterized for total concentration of elements using USEPA method 3051 and multi-elements analysis by ICP-OES [28]. Since chemical precipitation involves only dissolved inorganic P, all forms in sample were transformed into inorganic form where, to dissolve organic fraction of P, the wastewater was hydrolysed under reflux with hydrogen peroxide and hydrochloric acid to have 3% of pure H_2O_2 and 10% of concentrated HCl [44]. The experiments were conducted in batch reactors at room temperature 22 °C with variation of factors of pH, Ca:P, Mg:P and NH_4^+:P. The adjustment of pH was done using aqueous sodium hydroxide solution (6 M NaOH) and hydrochloric acid (1 M HCl) to exact pH ± 0.1. The molar ratio of calcium, magnesium and ammonium to P were adjusted by adding the pre-calculated quantity of their solution to samples to comply with molar ratio in design of experiments. In this case, ammonium chloride (4 $mol{\cdot}kg^{-1}$), dipotassium hydrogen phosphate (1 $mol{\cdot}kg^{-1}$), calcium chloride (1 $mol{\cdot}kg^{-1}$) and magnesium sulfate (2 $mol{\cdot}kg^{-1}$) were used. The 250 g of sample was brought to 400 g in reactor with deionized water after addition of all doses. The stirring rate was set at 60 rpm, reaction time of 60 min, and 1 h for liquid-solid phase equilibrium as described in other works [29,30]. Up to 2 mL sample was taken from liquid phase after equilibrium using a syringe and filtered immediately using membrane syringe filter 0.45 μm diameter, weighed and diluted for analysis of P in effluent phase. The phases were separated by filtration with vacuum pump and the washed precipitate was dried at room temperature. Phosphorus in the effluent was analysed using ICP-OES; while ammonium in dry precipitate was determined using EPA method 350.1 with modification. In summary for ammonium analysis, an aliquot weight (0.1–0.3 g) of solid precipitate was steam distilled in alkaline conditions, collected in boric acid containing mixed indicator, and titrated with 0.1 N HCl. The dry solid for optimized and non-optimized conditions were characterized using XRD and SEM following non-destructive methods (EN-13925 and ISO 22309:2011) for characterization of crystalline materials. Furthermore, the evaluation of products as fertilizer was done in citric acid 2% adjusted to pH 6 with KOH 5 N. In this case, 1 g of dry product was dissolved in 100 g citric acid solution as per referred work [31]; up to nine measurements of nutrients in each 0.22 μm dilute filtrate was done during two hours with time of 0, 1.5, 3, 9, 15,25, 50, 80, and 120 min [31,32].

2.5. Data analysis

Experiments were conducted in three level experimental design corresponding to low, middle and high levels coded by −1; 0; and +1, respectively. The number N of experiments was reduced to Box–Behnken design where $N = 2k^2 - 2k + c_p$, with c_p, center point replications, k is the number of factors [33]. Four factors were investigated including pH, mixing molar ratio of Mg:P, Ca:P and NH_4^+ excess on magnesium. The latter was a multiplication factor to Mg:P dose. The estimation of the pH range for experiments was based on sample composition and common proton transfer equilibria of solution components using their acidity constants. These include major conjugate acid-base pairs such as (i) phosphate conjugate pairs: $H_3PO_4/H_2PO_4^-$ (pK=2.15); $H_2PO_4^-/HPO_4^{2-}$ (pK=7.20); HPO_4^{2-}/PO_4^{3-} (pK=12.0), (ii) sulfate: H_2SO_4/HSO_4^- (pK = −1.98); HSO_4^-/SO_4^{2-} (pK=1.55), (iii)

carbonate: CO_2/H_2CO_3 (pK=1.47); H_2CO_3/HCO_3^- (pK = 6.35); HCO_3^-/CO_3^{2-}(pK=10.3), and (iv) ammonia pair: NH_4^+/NH_3 (pK = 9.25) [34,35]. The used molar fraction and proton dependent speciation model (α_i=$f(H^+)$) is given by Eq. (2).

$$\alpha_i = \frac{[H^+]^{n-i}K_0 \ldots K_i}{[H^+]^{n-0}K_0 + [H^+]^{n-1}K_1 + [H^+]^{n-2}K_1K_2 + \ldots + [H^+]^{n-n}K_1K_2 \ldots .K_n} \quad (2)$$

In that regard, good conditions are alkaline with experimental pH conditions of 8–11. Under these conditions, ammonium and HPO_4^{2-} are predominant with 10–90 percent of molar fraction in pH range 7.5–10, while PO_4^{3-} is predominant at 7–80% in pH range of 11–13. Thus, alkaline pH enhances supersaturation of P salts. In this context, factors corresponded to the lower level (−1) of 8, 0.5, 0.25 and 1; the middle level (0) was 9.5, 1, 0.625 and 2; while the high level (+1) was 11, 1.5, 1, and 3 for pH, Mg:P, Ca:P, and ammonium excess, respectively.

To assess the efficiency of P removal, the percentage of P recovery (X-Rec P) was calculated as fraction of feed P concentration which was precipitated (X-Rec P (%) = 100 x ($1-P_{out}/P_{in}$)). Struvite production was evaluated as a fraction of ammonium content (X-NH_4^+) in formed solid [36]. For both percentages of P recovery (X-Rec P) and struvite precipitation, polynomial models (Eq. (3)) with linear (x_i), quadratic (x_i^2) and interaction (x_ix_j) terms were used [33,37]. The parameters b_0, b_i, b_{ii}, b_{ij}, and e are intercept, linear, quadratic, interactions and error coefficients.

$$Y = b_0 + \sum_i^k b_i x_i + \sum_{i=1}^k b_{ii} x_i^2 + \sum_{i<j} \sum_j b_{ij} x_i x_j + e \quad (3)$$

Where two results were fractions of P recovery (X-Rec P) and struvite formation (X-NH_4^+), while independent variables are the experimental factors of pH, Mg:P mole ratio, Ca:P molar ratios and NH_4^+ excess. The optimization of two models, *X-Rec P* and X-NH_4^+, was based on maximizing desirability function d(y_i) described in Eq. (4) where Y_i is a given specified response, L_i is lower boundary, T is the target response. Weight parameters, s, are found based on eigen vectors of each response matrix [38,39]. By giving the same importance to all responses, the overall desirability D is obtained as geometric mean of each response desirability d_i in optimization process Eq. (5).

$$d(yi) = (Y_i - L_i/T - L_i)^s \quad (4)$$

$$D = (d_1 \cdot d_2 \cdot d_3 \cdot \ldots d_n)^{1/n} = \left(\prod_{i=1}^n d_i\right)^{1/n} \quad (5)$$

The closer to unit are d_i, the maximum will be D; otherwise any null d_i makes null overall desirability [34]. On stoichiometric point, the saturation index (*SI*) of possible P products was estimated from concentration of components in solution based on ion pairing activity products and the solubility products (*Ksp*) described in Eq. (6).

$$SI = logIAP - logKsp \quad (6)$$

With IAP, ion activity product, estimated by $IAP = \prod_i^N a_i^{zi}$ where a_i is activity of iterative ionic species i and corresponding^{i}stoichiometric coefficient, z_i [40]. Furthermore, in such multicomponent system, the precipitation of phosphate by different other species follows mass balance contribution where many compounds are assumed to co-precipitate (Eq. (7)) [41].

$$TOT_{PO_4^{3-}} = [PO_4^{3-}] + \sum_i^N v_{i,j} Z_j \quad (7)$$

With $TOT_{PO_4^{3-}}$, the total molal concentration of phosphate involved in the reaction system; $[PO_4^{3-}]$, phosphate concentration in solution, and the sum of N molal concentrations (Z_j) of phosphate binding components with v_i, stoichiometric coefficient that equals to the number of moles of PO_4^{3-} present in one mole of jth species. The data from precipitation experiments were analysed using Design Expert 12 software. In this tool, two responses were analysed and optimized separately by maximizing them and keeping all other factors in the range. The multi-response optimization was done by maximizing both responses, minimizing errors and keeping all factors in experimental range. On the other hand, Visual MINTEQ 3.1 was used for stoichiometric methods in ion pairing, *SI* estimation, and speciation of precipitate. The data obtained from experimental assay of product quality as a fertilizer in citric acid were studied as kinetic process. In this case, the release of nutrients in function of time were fitted to dissolution kinetic models [42]. The latter are diffusion dependent as described in Eq. (8).

$$-dC/dt = (C_s - C)/\delta \quad (8)$$

Where dc/dt is the variation of dissolved concentration over the change of time, C_s is the saturation concentration, C is the concentration at time t, and δ the thickness of solid–liquid interface diffusion layer. The Eq. (8) is changed to rate constant (k) Eq. (9) which integration from 0 to C in time from 0 to time t gives an exponential function (Eq. (10))

$$-dC/dt = k(C_s - C) \quad (9)$$

$$C = C_s\left(1 - e^{-kt}\right) \quad (10)$$

To assess the time required to reach a fraction of saturation, Eq. (10) is adapted to time constant (τ) expression (Eq. (11)).

$$C = C_s\left(1 - e^{-t/\tau}\right) \quad (11)$$

In fact, Eq. (11) considers the faster release in first step with limited time to saturation Cs and slow release in second step ($-dC/dt = 1/\tau \cdot C$) where the first order process starts to be counted [43]. The concentration of dissolved nutrients varies with time, where the time, t_x, required to have C as fraction X of Cs can be estimated from Eqs. (11) and (12).

$$t_x = -\tau \ln(1 - X) \quad (12)$$

With t_x in minutes, and X as a fraction number ranging from 0 to 1. The t_{80} was used to assess the time required for a product to reach 80 percent of the maximum nutrient release and played a role in comparative evaluation of struvite production under this study and usual chemical precipitation using calcium addition. The kinetic parameters for Eqs. (10) and (11) were estimated by rate constant and time constant exponential growth functions in originPro 2019.

3. Results and discussion

3.1. Characteristic results of whey

The analytical results of the sample for physical-chemical parameters of interest are presented in Table 1 and served in estimation of saturation indices *(SI)* for probable P precipitate. Trace elements were considered as Zn, Tl, Si, B, Sb, Mo, Ba, Ti, Ag, Mn, Al. Their concentrations were between 0.01 and 2.6 mg·kg^{-1}. Heavy metals included cadmium (0.002 mg·kg^{-1}), lead (1.08 mg·kg^{-1}) and chromium (0.204 mg·kg^{-1}). The concentrations of other transition metals were below limit of detection. The P concentration was higher than acceptable limits of effluents [44], while heavy metals concentrations are low and the wastewater can be used in P recycling [45].

In light of the elemental composition of wastewater, calcium, potassium, and ammonium have higher molal concentration than P. To find *SI* for P products to be formed by ion pairing with phosphate, only elements with the concentration higher than 0.1 mmol·kg^{-1} were used while those equal or below 0.1 mmol·kg^{-1} were considered as traces. The latter have molar ratio on P near to zero thus with

Table 1
Elemental composition of waste.

Analyte	Concentration	Molar ratio to P
K (mg·kg^{-1})	1640	1.87
Ca (mg·kg^{-1})	1310	1.45
P (mg·kg^{-1})	698	1.00
NH_4^+ (mg·kg^{-1})	600	1.48
Na (mg·kg^{-1})	490	0.95
Mg (mg·kg^{-1})	108	0.20
S (mg·kg^{-1})	88.2	0.12
NO_2^- (mg·kg^{-1})	8.93	–
NO_3^- (mg·kg^{-1})	200	–
SO_4^{2-} (mg·kg^{-1})	0.75	–
pH	4.35	–
Density	1.02	–
Tot. N (%)	0.1	–
Tot. C (%)	1.81	–
Org. C (%)	1.21	–

negligible contribution in phosphate precipitation. The obtained SI values in relation to phosphate are presented in Table 2.

Considering the obtained *SI*, calcium and magnesium are the main phosphate counterions with positive *SI* thus possibility of co-precipitation. Furthermore, calcium phosphate salts have higher *SI* than struvite. This suggests possible inhibition of struvite precipitation. Thus optimizing struvite precursors in reactor is the main way of overcoming more stable calcium phosphate precipitates. The design of experiments aimed to overcome the effect of calcium and enhance struvite precipitation at high concentration.

3.2. Results of experiments

The number of experiments was calculated to 27 runs. These included 24 experiments and 3 replications of center point.

The studied factors in coded and their actual values together with the results of P recovery, X-Rec P, and ammonium content, X-NH_4^+, in dry solid are presented in Table 3 while the resulting experimental model parameters are presented in Table 4. Models were fitted with determination coefficients R^2 = 0.96 and 0.95 for P recovery and struvite precipitation, respectively. Their *F*-values were larger than critical value ($F_{stat} > F_{crit}$) and $p < 0.05$ which suggest their fitting significance. In addition, the difference between adjusted and predicted R^2 was smaller than 0.2 and non-significant lack of fit ($p > 0.05$). In consideration of aforementioned fitting parameters, the experimental models fulfil the main criteria of usefulness in prediction of results of P recovery and struvite precipitation.

Considering the effects, all factors are linearly significant in P recovery and struvite precipitation ($p < 0.05$). By model reduction, the significant interactions ($p < 0.1$) included pH·(Ca:P) for P recovery (Fig. 1a) where the increase of both pH and Ca:P enhances P recovery, while the latter factor decreased significantly struvite production (Fig. 1b).

Table 3
Experimental results of P recovery and ammonium content in solid phase.

	Factors coded and actual in ()				Responses	
n°	pH	Mg:P	Ca:P	NH_4^+excess	X-Rec P (%)	X-NH_4^+ (%)
1	−1 (8)	+1 (1.5)	0 (0.625)	0 (2)	76.6	4.50
2	0 (9.5)	+1 (1.5)	0 (0.625)	−1 (1)	94.5	4.13
3	+1 (11)	0 (1)	0 (0.625)	+1 (3)	90.5	2.05
4	0 (9.5)	+1 (1.5)	+1 (1)	0 (2)	94.0	3.13
5	0 (9.5)	−1 (0.5)	0 (0.625)	−1 (1)	74.8	1.30
6	0 (9.5)	0 (1)	0 (0.625)	0 (2)	93.8	4.13
7	+1 (11)	−1 (0.5)	0 (0.625)	0 (2)	76.3	0.56
8	0 (9.5)	−1 (0.5)	−1 (0.25)	0 (2)	72.3	4.29
9	−1 (8)	0 (1)	0 (0.625)	+1 (3)	78.3	4.10
10	−1 (8)	0 (1)	0 (0.625)	−1 (1)	72.3	2.91
11	−1 (8)	0 (1)	+1 (1)	0 (2)	69.1	2.44
12	+1 (11)	0 (1)	0 (0.625)	−1 (1)	94.2	0.44
13	0 (9.5)	0 (1)	0 (0.625)	0 (2)	96.0	3.24
14	+1 (11)	+1 (1.5)	0 (0.625)	0 (2)	95.6	1.15
15	0 (9.5)	0 (1)	0 (0.625)	0 (2)	96.5	2.93
16	0 (9.5)	+1 (1.5)	−1 (0.25)	0 (2)	98.6	5.92
17	+1 (11)	0 (1)	−1 (0.25)	0 (2)	97.3	1.32
18	0 (9.5)	0 (1)	−1 (0.25)	+1 (3)	97.6	5.60
19	0 (9.5)	0 (1)	−1 (0.25)	−1 (1)	97.7	4.38
20	0 (9.5)	0 (1)	+1 (1)	+1 (3)	93.0	2.20
21	0 (9.5)	+1 (1.5)	0 (0.625)	+1 (3)	96.4	4.88
22	−1 (8)	0 (1)	−1 (0.25)	0 (2)	90.0	6.37
23	−1 (8)	−1 (0.5)	0 (0.625)	0 (2)	59.8	1.95
24	+1 (11)	0 (1)	+1 (1)	0 (2)	90.8	0.27
25	0 (9.5)	−1 (0.5)	0 (0.625)	+1 (3)	77.8	1.88
26	0 (9.5)	0 (1)	+1 (1)	−1 (1)	92.1	0.96
27	0 (9.5)	−1 (0.5)	+1 (1)	0 (2)	78.1	0.46

Table 4
Summary of parameters in experimental models.

Parameters /terms	X-Rec P			X-NH_4^+		
	bi,j	*F*-value	*P*-value	bi,j	*F*-value	*P*-value
Intercept	−391	20	< 0.01	−26.5	17	< 0.01
pH	+84.9	74	< 0.01	+7.31	70	< 0.01
pH^2	−4.26	44.7	< 0.01	−0.45	17.6	0.01
(Mg:P)	+93.9	103	< 0.01	+9.36	45.3	< 0.01
$(Mg:P)^2$	−36.4	40.3	< 0.01	−0.99	0.10	0.76
(Ca:P)	−59.2	10.1	<0.01	−19	87.4	< 0.01
$(Ca:P)^2$	+2.67	0.07	0.8	+1.08	0.08	0.78
(NH_4^+)	+20.3	0.49	0.5	−0.45	11.2	< 0.01
(NH_4^+)^2	−1.04	0.53	0.48	−0.16	0.64	0.44
pH⍁(Mg:P)	+0.85	0.15	0.71	−0.65	2.96	0.11
pH⍁(Ca:P)	+6.34	4.62	0.05	+1.28	6.38	0.03
(Mg:P)⍁(Ca:P)	−13.7	2.42	0.15	+1.38	0.83	0.38
pH⍁(NH_4^+)	−1.62	2.14	0.17	+0.07	0.14	0.72
(Mg:P)⍁(NH_4^+)	−0.53	0.03	0.87	+0.08	0.02	0.88
(Ca:P)⍁(NH_4^+)	+0.69	0.02	0.88	+0.01	0.00	0.99
R^2	0.96				0.95	
F	20				17	
P	<0.01				<0.01	
$F_{crit,\ \alpha=0.05}$	2.53				2.53	

Table 2
Stoichiometric matrix of phosphate with its possible countercharge and related saturation index (SI).

Product	Stoichiometry							log IAP	SI
	K^+	H^+	Ca^{2+}	Mg^{2+}	NH_4^+	PO_4^{3-}	H_2O		
$MgHPO_4·3H_2O$(s)		1		1		1	3	−18.75	−0.58
K-struvite	1			1		1	6	−10.78	0.22
$CaHPO_4·2H_2O$(s)		1	1			1	2	−18.24	0.76
$Mg_3(PO_4)_2$(s)				3		2		−22.37	0.91
$CaHPO_4$(s)		1	1			1		−18.22	1.05
Struvite				1	1	1	6	−11.23	2.03
$Ca_3(PO_4)_2$			3			2		−20.85	8.07
$Ca_4H(PO_4)_3·3H_2O$(s)		1	4			3	3	−39.10	8.86
Hydroxyapatite		−1	5			3	1	−23.48	20.85

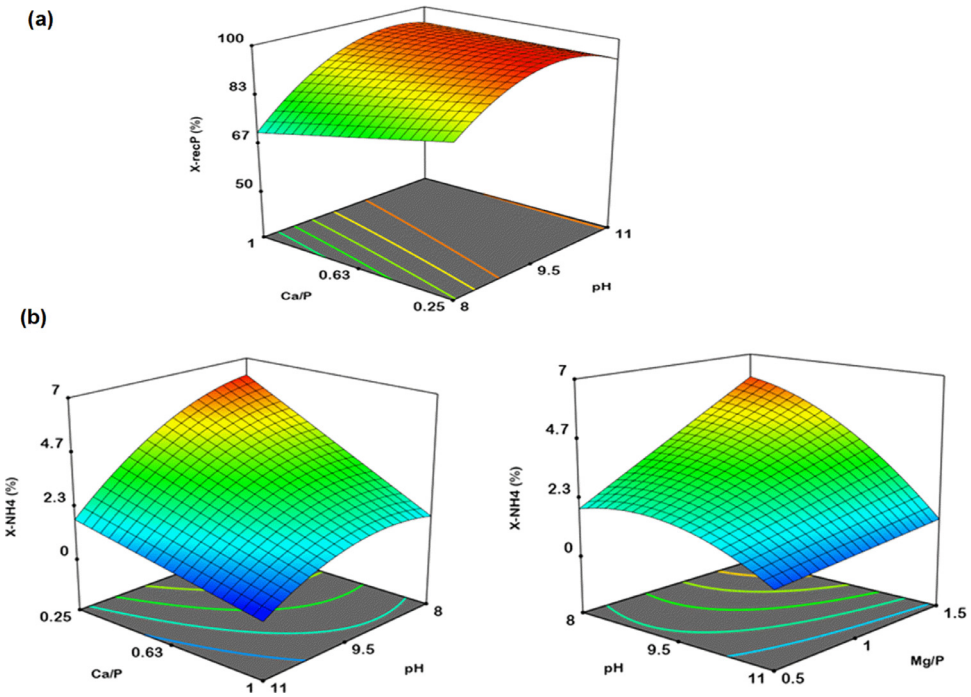

Fig. 1. Highlight of factors interactions on P recovery (a) and struvite precipitation (b).

The additional interaction of pH·(Mg:P) was significant in struvite formation. In fact, the increase of pH with Mg:P and Ca:P molar ratio enhances P recovery.

With regard to calcium supply, the ammonium is precipitated with decreased calcium dose. This suggests the lowered calcium phosphate precipitation potential and the favor to its counterpart, struvite. The rise in X-NH_4^+ with Mg:P is due to the super-saturation of struvite, which consequently increases its fraction in solid solution (Fig. 1b). To find out the best process conditions, each of the obtained models was optimized and three conditions are obtained. In fact, the optimum reaction conditions to recover maximum P by precipitation were found at pH 10.4 with Mg:P of 1.32, Ca:P of 0.77 and the ammonium excess of 1.19·Mg:P. The predicted percentage of P recovery is 98.7 ± 1.2 percent. Following the used high Ca:P dose, the struvite is decreased in formed P product. In fact, the proton transfer dynamic equilibrium of ammonium estimated by Eq. (2) highlights the decrease of ammonium and the adverse increase of ammonia form (> 60 per cent) at pH 10.4 starting to evolve from the reactor in the presence of strong base.

For struvite, the optimum X-NH_4^+ is found at pH 8.3, with dosage of 1.26, 0.25 and 1.84 as Mg:P, Ca:P and ammonium excess, respectively. The P product is characterized with high content of ammonium nitrogen which predicted X-NH_4^+ was 6.6 ± 0.2 percent, equivalent to 90.4 ± 3.2 percent of struvite. However, under these process conditions the P is less efficiently removed from wastewater estimated to 92 percent. In this regard, both P recovery and struvite production were found under multi-response optimization of both X-Rec P and X-NH_4^+. This was achieved with overall desirability D = 0.995 and optimum conditions of pH 8.9; molar ratios of 1.21, 0.26, and 2.22 for Mg:P, Ca:P, and ammonium excess, respectively. In these conditions, P is efficiently removed and struvite produced effectively. The predicted P recovery is 98.6 ± 1.1 percent while predicted ammonium fraction is 6.3 ± 0.2 percent equivalent to 85.7 ± 2.5 percent of struvite content in the product.

The importance of the current work was relevant in struvite enhancement during P precipitation. In fact, the mass contribution balance Eq. (7) was implemented in Visual MinteQ 3.1 and demonstrated the spontaneous precipitation of P in alkaline pH without additional salts. However, the favored product is calcium salt of hydroxyapatite thus without good quality for use as fertilizer. Two operational conditions mitigate the struvite inhibition problem which include struvite and multi-response optimum conditions obtained in this study. Given that the solid phase speciation shows mainly a binary solid mixture of struvite and hydroxyapatite, and the predominant HPO_4^{2-} species of P at pH 8.9, the favored equilibrium reactions for struvite crystallization and the main amorphous salt can be described by Eqs. (13)) and ((14), respectively.

$$Mg^{2+}_{(aq)} + NH_4^+_{(aq)} + HPO_4^{2-}_{(aq)} + 6H_2O_{(l)} \rightleftharpoons MgNH_4PO_4\ 6H_2O\ (s) + H^+_{(aq)} \quad (13)$$

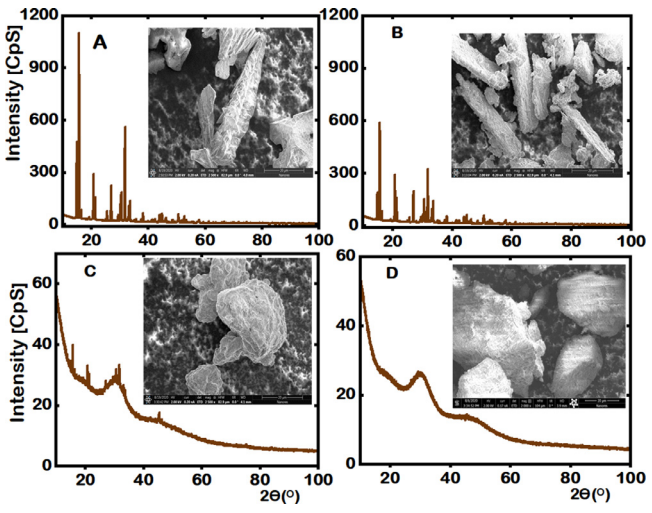

Fig. 2. XRD spectra and corresponding SEM images (20 μm scale, 2000–2500 magnification) of crystalline aspect of recovered products A: Optimum for struvite precipitation (X-NH_4^+); B: Product of multi-response optimum conditions (Both X-NH_4^+ and X-Rec P); C: Product of optimum P recovery, and D: Precipitate at pH 8.9 without additional salt.

Table 5
Elemental composition of the products.

Elements	Recovered P products		
	A	B	C
N (%)	5.40 ± 0.2	5.00 ± 0.2	1.40 ± 0.2
P_2O_5 (%)	29.3 ± 1.1	28.7 ± 0.4	23.2 ± 0.8
K (%)	0.80 ± 0.1	1.00 ± 0.1	0.70 ± 0.1
Ca (%)	0.72 ± 0.1	1.04 ± 0.1	9.30 ± 0.3
Mg (%)	9.60 ± 0.1	9.40 ± 0.6	2.60 ± 0.5
Hg, As, Pb, Cd (mg kg^{-1})	< 2	< 2	< 2

$$5Ca^{2+}_{(aq)} + 3HPO_{4(aq)}^{2-} + H_2O_{(l)} \rightleftharpoons Ca_5(PO_4)_3(OH)(s) + 4H^+_{(aq)} \quad (14)$$

The formation of struvite and amorphous salt of hydroxyapatite is in accordance with other works [46]. For comparative study, three products were experimentally formed. These include the product A produced under optimum conditions enhancing struvite crystallization, product B formed in conditions of both P removal and struvite production, and product C obtained in conditions of maximum P recovery with high dose of calcium salts. In three production processes, A was produced with P removal of 92 percent and 6.9 ± 0.3 percent of ammonium content in precipitate i.e. 94.5 ± 4.1 percent of struvite crystallization. The production of B, improved the P recovery with 96 percent and 6.5 percent of ammonium content in the product equivalent to 89 percent of struvite content. The production of C, also demonstrated a P recovery of 96 percent and lower content of ammonium. The latter was 1.7 percent equivalent to 23 percent of struvite content. In fact, C production involves high calcium dose in substrate and is hereby considered as equivalent to applied processes of chemical precipitation with calcium addition for P removal in WWTP. The

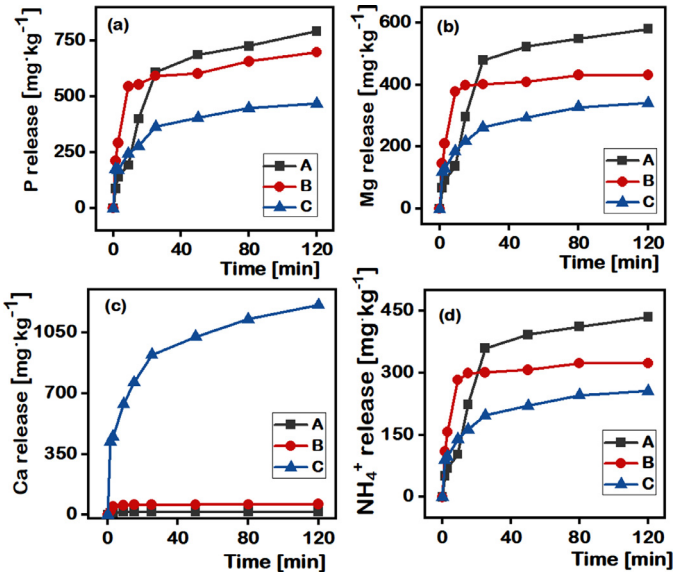

Fig. 3. In-vitro assay of nutrient release in citric acid (a): P release, (b) Mg release, (c): Ca release and (d): NH_4^+ release.

deficit is the lower quality of precipitate in fertilizer (see Section 3.3). Thus process conditions in A and B produce P products with both P and nitrogen at higher concentrations. The application of process B is effective in P removal and struvite precipitation from wastewater containing high calcium concentration. The use of lower Ca:P complies with previous research that recommended to keep Ca:P < 0.5 for the favor of struvite [16], and pH below 9.5 [47]. Compared to the

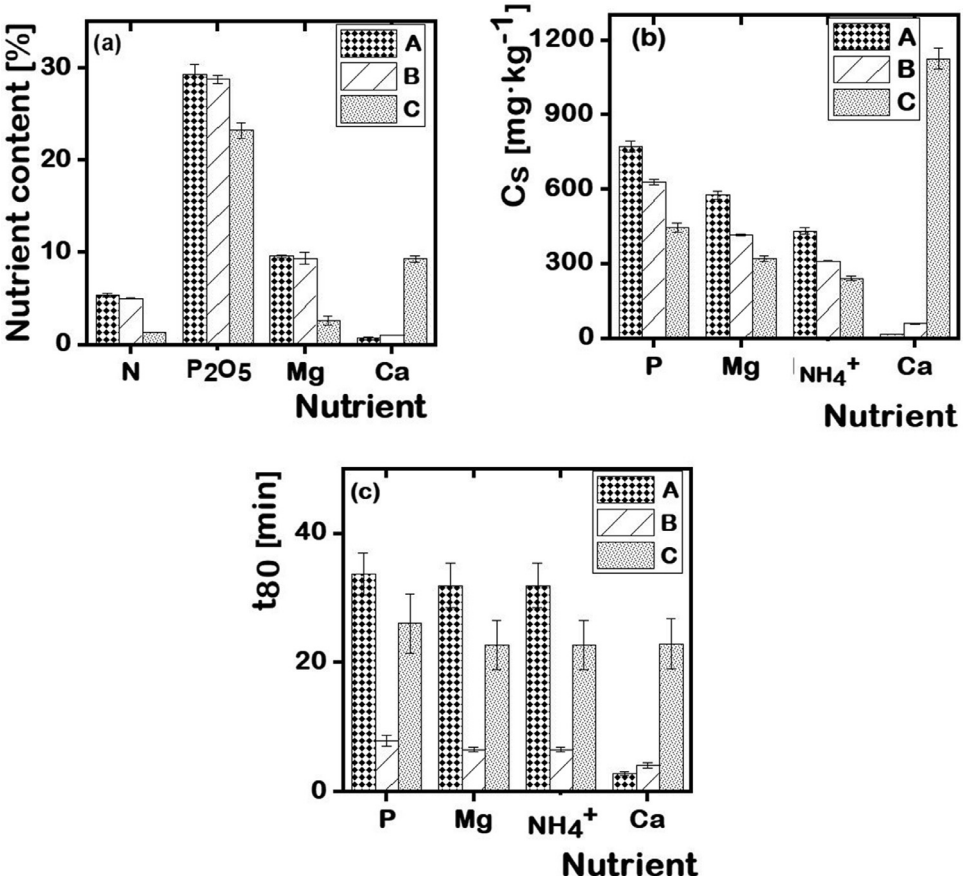

Fig. 4. Comparison of (a) nutrient content in three phosphorus products, (b) nutrient availability (c) nutrient t_{80}.

Table 6
Kinetic parameters of nutrient release.

Model	Products	Kinetic parameters Eqs. (10) and (11)			Eq. (12) Time constante model	
		Cs[mgkg^{-1}]	k [min^{-1}]	R^2	τ	t_{80}
P release	**A**	773 ± 21	0.05 ± 0.01	0.990	21.0 ± 2	33.8 ± 3.2
	B	630 ± 12	0.20 ± 0.02	0.999	4.90 ± 0.53	7.90 ± 0.9
	C	446 ± 17	0.06 ± 0.01	0.984	16.2 ± 2.8	26.1 ± 4.6
Mg Release	**A**	576 ± 18	0.05 ± 0.01	0.995	19.9 ± 2.1	32.0 ± 3.5
	B	416 ± 4.0	0.25 ± 0.01	0.999	4.10 ± 0.2	6.50 ± 0.3
	C	322 ± 12	0.07 ± 0.01	0.994	14.1 ± 2.3	22.7 ± 3.8
NH_4^+ release	**A**	432 ± 13	0.05 ± 0.01	0.995	19.9 ± 2.1	32.0 ± 3.5
	B	312 ± 3.0	0.25 ± 0.01	0.999	4.10 ± 0.2	6.50 ± 0.3
	C	241 ± 9.0	0.07 ± 0.01	0.994	14.1 ± 2.3	22.7 ± 3.8
Ca release	**A**	16.2 ± 0.2	0.56 ± 0.04	0.979	1.80 ± 0.1	2.80 ± 0.2
	B	58.9 ± 1.0	0.39 ± 0.04	0.968	2.60 ± 0.3	4.10 ± 0.4
	C	1130 ± 41	0.07 ± 0.01	0.981	14.2 ± 2.4	22.9 ± 3.9

product C, the obtained products A and B are crystalline as viewed in SEM (Fig. 2A–C). The orthorhombic structures of products A and B are witness of struvite crystallization. The increased Ca:P affects crystal morphology up to deformation (Fig. 2C, and D).

Moreover, the pattern with XRD struvite was found for both production conditions of pH 8.3 (product A) and multi-response conditions of pH 8.9 (product B) as shown on Fig. 2A and B, respectively. The crystalline salts thereby formed were confirmed to be 100% struvite by XRD characterization. In contrast, Fig. 2C as well as Fig. 2D show the formation of amorphous phase predominant in solid product which composition were not confirmed in XRD characterization. Furthermore, pH above 10 required high quantity of alkali addition to increase pH due to buffering system in range of pH 8–10. The main buffer equilibrium is ammonium buffer (NH_4^+/NH_3, pH = 8.2–10.2) with maximum capacity at its pKa nearly pH 9.25 following the addition of ammonium to enhance struvite supersaturation [35]. Thus, the decrease in ammonium at pH > 10 shortens struvite precipitation while excess of the needed alkali renders the process more expensive. When no acid digestion is used, the pH in production of A and B are easier to achieve with small amount of alkali addition. Therefore, the doses obtained in B can be coupled to wastewater treatment with proper pH adjustment to favor struvite production.

3.3. Evaluation of product quality as fertilizer

Three products are compared for nutrient contents and their availability for plant nutrition by *in*-vitro study. The elemental composition of dry products in three experimental conditions (A, B and C) are summarized in Table 5. The high content in P and nitrogen for A and B makes them better P fertilizers than C.

For evaluation of P availability to plant, the results from real time measurements of *in*-vitro nutrients release in 2% citric acid with pH 6 are compared on Fig. 3a–d.

For three products, the nutrients release fit to exponential increase of first order kinetic models including rate constant and time constant expressions (Eqs. (10) and (11), respectively) which parameters are presented in Table 6.

The product C was characterized by lower nutrients' availability where Cs of P, Mg, NH_4^+ are significantly lower thus less available to plant. The visible highlights on Fig. 3a–d are the benefits of struvite production where nutrients are better released by A and B than C. The latter is basically rich in calcium phosphate and is characterized by low P availability. The former two products diffuse P, magnesium and nitrogen to solution and reach higher Cs. The findings are in agreement with products nutrients levels (Fig. 4a), where A and B are characterized by higher P, magnesium and nitrogen contents. Besides the high P availability (C_s) provided by A as shown on Fig. 4b, it has a slow nutrient release properties than others. Considering t_{80}, the product A required longer time to release 80% of Cs. Fig. 4(c) shows that t_{80} of P, ammonium, and magnesium release are significantly higher in A than in other products.

The property of slow nutrient release was previously reported for struvite and qualifies it as an efficient fertilizer [48]. However, the higher efficiency in P removal can be achieved by production of B which also demonstrated high nutrients' availability.

4. Summary and conclusion

The recovery of phosphorus as struvite from dairy processing wastewater was possible upon design of experiments and optimization. The optimum conditions for both P recovery and struvite production were found at pH 8.9 with mixing molar ratio of 1.21, 0.26, 2.69 for Mg:P, Ca:P and NH_4^+:P, respectively. In these conditions, the phosphate counter-charged elements that mainly included calcium have precipitated with struvite at minimized level. The P is efficiently removed with predicted and experimental removal of 98.6 ± 1.1 and 96 percent, respectively. The predicted and experimental struvite content in B was 85.7 ± 2.5, and 89 percent, respectively. The product is rich in P and nitrogen with their efficient release to plant nutrition. Furthermore, in application of developed model, searching for cost and environmental effective magnesium and ammonium sources are subsequent activities of research in struvite production from dairy processing wastes.

Symbols

P: Phosphorus
MAP: Magnesium Ammonium Phosphate Hexahydrate
WWTP : Waste Water Treatment Plant
K_{sp} : Solubility product
ICP-OES: Inductively Coupled Plasma Optical Emission Spectroscopy
SEM: Scanning Electron Miscroscopy
XRD: X-Ray Diffraction
EPA: Environmental Protection Agency
IAP: Ion Activity Product
D: Desirability
CpS: Counts per Second

Declaration of Competing Interest

None.

Acknowledgment

This work was financially supported by REFLOW project (Phosphorus recovery for fertilizers from dairy processing wastes), H2020 MSC-ITN grant number 814258.

Supplementary materials

Supplementary material associated with this article can be found, in the online version, at doi:10.1016/j.jtice.2020.11.031.

References

[1] Amann A, Zoboli O, Krampe J, Rechberger H, Zessner M, Egle L. Environmental impacts of phosphorus recovery from municipal wastewater. Resour Conserv Recycl 2018;130:127–39. doi: 10.1016/j.resconrec.2017.11.002.

[2] Childers DL, Corman J, Edwards M, Elser JJ. Sustainability challenges of phosphorus and food: solutions from closing the human phosphorus cycle. Bioscience 2011;61:117–24. doi: 10.1525/bio.2011.61.2.6.

[3] Z XT, Lal R, Wiebe KD. Global soil nutrient depletion and yield reduction. J Sustain Agric 2005;26:123–46. doi: 10.1300/J064v26n01_10.

[4] Sharpley AN, Chapra SC, Wedepohl R, Sims JT, Daniel TC, Reddy KR. Managing agricultural phosphorus for protection of surface waters: issues and options. J Environ Qual 1994;23:437–51. doi: 10.2134/jeq1994.00472425002300030006x.

[5] Jarvie HP, Neal C, Withers PJA. Sewage-effluent phosphorus: a greater risk to river eutrophication than agricultural phosphorus? Sci Total Environ 2006;360:246–53. doi: 10.1016/j.scitotenv.2005.08.038.

[6] Correll DL. The role of phosphorus in the eutrophication of receiving waters: a review. J Environ Qual 1998;27:261–6. doi: 10.2134/jeq1998.00472425002700020004x.

[7] Bunce JT, Ndam E, Ofiteru ID, Moore A, Graham DW. A review of phosphorus removal technologies and their applicability to small-scale domestic wastewater treatment systems. Front Environ Sci 2018;6:1–15. doi: 10.3389/fenvs.2018.00008.

[8] Clark T, Stephenson T, Pearce PA. Phosphorus removal by chemical precipitation in a biological aerated filter. Water Res 1997;31:2557–63. doi: 10.1016/S0043-1354(97)00091-2.

[9] Weeks JJ, Hettiarachchi GM. A review of the latest in phosphorus fertilizer technology: possibilities and pragmatism. J Environ Qual 2019;48:1300–13. doi: 10.2134/jeq2019.02.0067.

[10] Daneshgar S, Callegari A, Capodaglio AG, Vaccari D. The potential phosphorus crisis: resource conservation and possible escape technologies: a review. Resources 2018;7. doi: 10.3390/resources7020037.

[11] Antonilli M, Bottari E, Festa MR, Gentile L. Complex formation between arginine and calcium (II) and magnesium (II). Chem Speciat Bioavailab 2009;21:33–40. doi: 10.3184/095422909×418502.

[12] Maneedaeng A, Flood AE, Haller KJ, Grady BP. Modeling of precipitation phase boundaries in mixed surfactant systems using an improved counterion binding model. J Surfactants Deterg 2012;15:523–31. doi: 10.1007/s11743-012-1353-0.

[13] Bell LC, Mika H, Kruger BJ. Synthetic hydroxyapatite-solubility product and stoichiometry of dissolution. Arch Oral Biol 1978;23:329–36. doi: 10.1016/0003-9969(78)90089-4.

[14] Kazadi Mbamba C, Tait S, Flores-Alsina X, Batstone DJ. A systematic study of multiple minerals precipitation modelling in wastewater treatment. Water Res 2015;85:359–70. doi: 10.1016/j.watres.2015.08.041.

[15] Taylor P, Afolabi TJ, Alade AO, Jimoh MO, Fashola IO. Heavy metal ions adsorption from dairy industrial wastewater using activated carbon from milk bush kernel shell n.d. https://doi.org/10.1080/19443994.2015.1074619.

[16] Huchzermeier MP, Tao W. Overcoming challenges to struvite recovery from anaerobically digested dairy manure. Water Environ Res 2012;84:34–41. doi: 10.2175/106143011×13183708018887.

[17] Shalaby MS, El-Rafie S, Hamzaoui AH, M'nif A. Modeling and optimization of phosphate recovery from industrial wastewater and precipitation of solid fertilizer using experimental design methodology. Chem Biochem Eng Q 2015;29:35–46. doi: 10.15255/CABEQ.2014.2107.

[18] Wang J, Burken JG, Zhang X, Surampalli R. Engineered struvite precipitation: impacts of component-ion molar ratios and pH. J Environ Eng 2005;131:1433–40. doi: 10.1061/(ASCE)0733-9372(2005)131:10(1433).

[19] Marti N, Bouzas A, Seco A, Ferrer J. Struvite precipitation assessment in anaerobic digestion processes. Chem Eng J 2008;141:67–74. doi: 10.1016/j.cej.2007.10.023.

[20] Bennett AM, Lobanov S, Koch FA, Mavinic DS. Improving potassium recovery with new solubility product values for K-struvite. J Environ Eng Sci 2017;12:93–103. doi: 10.1680/jenes.17.00019.

[21] Kataki S, West H, Clarke M, Baruah DC. Phosphorus recovery as struvite from farm, municipal and industrial waste: feedstock suitability, methods and pretreatments. Waste Manag 2016;49:437–54. doi: 10.1016/j.wasman.2016.01.003.

[22] Wei SP, van Rossum F, van de Pol GJ, Winkler MKH. Recovery of phosphorus and nitrogen from human urine by struvite precipitation, air stripping and acid scrubbing: a pilot study. Chemosphere 2018;212:1030–7. doi: 10.1016/j.chemosphere.2018.08.154.

[23] Castro LDP, Vecino-Gutierrez KP, Díaz-Moyano LJ, Jaimes-Estévez J, Escalante-Hernández H. Lighting the anaerobic digestion process in rural areas: obtainment of struvite from bovine manure digestate. Rev Colomb Biotecnol 2018;20:78–88. doi: 10.15446/rev.colomb.biote.v20n2.71184.

[24] Matynia A, Wierzbowska B, Hutnik N, Mazienczuk A, Kozik A, Piotrowski K. Separation of struvite from mineral fertilizer industry wastewater. Procedia Environ Sci 2013;18:766–75. doi: 10.1016/j.proenv.2013.04.103.

[25] Kwon G, Kang J, Nam JH, Kim YO, Jahng D. Recovery of ammonia through struvite production using anaerobic digestate of piggery wastewater and leachate of sewage sludge ash. Environ Technol 2018;39:831–42. doi: 10.1080/09593330.2017.1312550.

[26] Kapsak WR, Rahavi EB, Childs NM, White C. Functional foods: consumer attitudes, perceptions, and behaviors in a growing market. J Am Diet Assoc 2011;111:804–10. doi: 10.1016/j.jada.2011.04.003.

[27] Birnhack L, Nir O, Telzhenski M, Lahav O. A new algorithm for design, operation and cost assessment of struvite (MgNH4PO4) precipitation processes. Environ Technol 2015;36:1892–901. doi: 10.1080/09593330.2015.1015455.

[28] Vudagandla S, Siva Kumar N, Dharmendra V, Asif M, Balaram V, Zhengxu H, et al. Determination of boron, phosphorus, and molybdenum content in biosludge samples by microwave plasma atomic emission spectrometry (MP-AES). Appl Sci 2017;7:264. doi: 10.3390/app7030264.

[29] Shaddel S, Grini T, Ucar S, Azrague K, Andreassen JP, Østerhus SW. Struvite crystallization by using raw seawater: improving economics and environmental footprint while maintaining phosphorus recovery and product quality. Water Res 2020;173:115572. doi: 10.1016/j.watres.2020.115572.

[30] Shalaby MS, El-Rafie S, Hamzaoui AH, M'nif A. Modeling and optimization of phosphate recovery from industrial wastewater and precipitation of solid fertilizer using experimental design methodology. Chem Biochem Eng Q 2015;29:35–46. doi: 10.15255/CABEQ.2014.2107.

[31] Thant Zin MM, Kim DJ. Struvite production from food processing wastewater and incinerated sewage sludge ash as an alternative N and P source: optimization of multiple resources recovery by response surface methodology. Process Saf Environ Prot 2019;126:242–9. doi: 10.1016/j.psep.2019.04.018.

[32] Santos W.O. Acid Ammonium citrate as p extractor for fertilizers of varying solubility 2019:1–12.

[33] Polat S, Sayan P. Application of response surface methodology with a Box–Behnken design for struvite precipitation. Adv Powder Technol 2019;30:2396–407. doi: 10.1016/j.apt.2019.07.022.

[34] Loewenthal RE, UR K, EP van H. Modellingstruvite_precipitation. Water Sci Technol 1994;30:107–16.

[35] Barnes NJ, Bowers AR. A probabilistic approach to modeling struvite precipitation with uncertain equilibrium parameters. Chem Eng Sci 2017;161:178–86. doi: 10.1016/j.ces.2016.12.026.

[36] Capdevielle A, Sýkorová E, Biscans B, Béline F, Daumer ML. Optimization of struvite precipitation in synthetic biologically treated swine wastewater – determination of the optimal process parameters. J Hazard Mater 2013;244–245:357–69. doi: 10.1016/j.jhazmat.2012.11.054.

[37] Numviyimana C, Chmiel T, Kot-Wasik A, Namieśnik J. Study of pH and temperature effect on lipophilicity of catechol-containing antioxidants by reversed phase liquid chromatography. Microchem J 2019;145. doi: 10.1016/j.microc.2018.10.048.

[38] John B. Application of desirability function for optimizing the performance characteristics of carbonitrided bushes. Int J Ind Eng Comput 2013;4:305–14. doi: 10.5267/j.ijiec.2013.04.003.

[39] Varala S, Dharanija B, Satyavathi B, Basava Rao VV, Parthasarathy R. New biosorbent based on deoiled karanja seed cake in biosorption studies of Zr(IV): optimization using Box-Behnken method in response surface methodology with desirability approach. Chem Eng J 2016;302:786–800. doi: 10.1016/j.cej.2016.05.088.

[40] Baeza Baeza JJ, Ramis-Ramos G. A series expansion of the extended Debye-Huckel equation and application to linear prediction of stability constants. Talanta 1996;43:1579–87. doi: 10.1016/0039-9140(96)01942-X.

[41] Eggermont SGF, Prato R, Dominguez-Benetton X, Fransaer J. Metal removal from aqueous solutions: insights from modeling precipitation titration curves. J Environ Chem Eng 2020;8:103596. doi: 10.1016/j.jece.2019.103596.

[42] Mathematical models of drug release. In: Bruschi ML, editor. Strategies to Modify the Drug Release from Pharmaceutical Systems. Elsevier; 2015. p. 63–86. doi: 10.1016/B978-0-08-100092-2.00005-9.

[43] Scholz G, Scholz F. First-order differential equations in chemistry. J Comput Sci Technol 2014;1. doi: 10.1007/s40828-014-0001-x.

[44] Almuktar SAAAN, Abed SN, Scholz M. Wetlands for wastewater treatment and subsequent recycling of treated effluent: a review. Environ Sci Pollut Res 2018;25:23595–623. doi: 10.1007/s11356-018-2629-3.

[45] Mansourri G, Madani M. Examination of the level of heavy metals in wastewater of bandar abbas wastewater treatment plant 2016:55–61.

[46] Moragaspitiya C, Rajapakse J, Millar GJ. Effect of Ca:Mg ratio and high ammoniacal nitrogen on characteristics of struvite precipitated from waste activated sludge digester effluent. J Environ Sci 2019;86:65–77. doi: 10.1016/j.jes.2019.04.023.

[47] Daneshgar S, Buttafava A, Capsoni D, Callegari A, Capodaglio AG. Impact of pH and ionic molar ratios on phosphorous forms precipitation and recovery from different wastewater sludges. Resources 2018;7. doi: 10.3390/resources7040071.

[48] Talboys PJ, Heppell J, Roose T, Healey JR, Jones DL, Withers PJA. Struvite: a slow-release fertiliser for sustainable phosphorus management? 2016:109–23. https://doi.org/10.1007/s11104-015-2747-3.